Dual-Frequency Folded Reflectarray Antenna

Jinjing Ren and Wolfgang Menzel, *Fellow, IEEE*

***Abstract*—Design and experimental results of a dual-frequency folded reflector antenna are presented. With an effective diameter of 180 mm and a depth of 60 mm, gain values of 25 and 30 dB at 20 and 30 GHz, respectively, have been achieved. Beamwidths are 6.2° at 20 GHz and 3.7°/4° at 30 GHz.**

***Index Terms*—Antennas, dual-frequency antennas, planar arrays, reflectarray.**

I. Introduction

A NUMBER of microwave systems use different frequencies at the same time, e.g., VSAT links with the downlink and uplink in the 20- and 30-GHz frequency range, respectively. A low-cost realization of reflector antennas can be done by simple printed reflectarrays. Dual-frequency reflectarrays have already been realized based on multilayer structures [1]–[4], by arranging separate elements for the two frequencies side by side [5], or using elements working at different frequencies in the two polarizations [3]–[5]. Finally, in [7], the reflector elements are switched between operating frequencies by p-i-n diodes. Recently, two approaches for single-layer dual-frequency reflectarrays for arbitrary polarizations have been presented [8], [9]. All these approaches, however, need a feed in front of the reflector. A way out of this problem has been demonstrated by folded reflectarray antennas for a single frequency band [6], [10].

In this letter, the folded reflectarray antenna principle is extended to the operation at two separate frequencies. As example frequencies, 20 and 30 GHz have been selected. The applied principle is similar to that used in [8] and [9], however the complication now is that dual-frequency operation must be maintained for two polarizations while adjusting a phase difference of 180° between the two at each frequency (see Section II).

In Section II, a short review of the folded reflectarray principle is given, followed by the approach for the reflector elements for a dual-frequency array. Finally, array design and experimental results are given.

II. Principle of a Folded Reflectarray Antenna

The principle cross section of a folded reflectarray is given in Fig. 1. A wave from the feed horn is incident on a polarizing grid with a polarization such that the wave is reflected back to the planar reflectarray that, at the same time, adjusts the necessary absolute phase angle to form a plane wave and provides

Manuscript received September 09, 2013; accepted September 18, 2013. Date of publication September 23, 2013; date of current version October 08, 2013.

The authors are with the Department of Microwave Techniques, University of Ulm, Ulm 89069, Germany (e-mail: Jinjing.Ren@uni-ulm.de; wolfgang.menzel@ieee.org).

Color versions of one or more of the figures in this letter are available online at http://ieeexplore.ieee.org.

Digital Object Identifier 10.1109/LAWP.2013.2283085

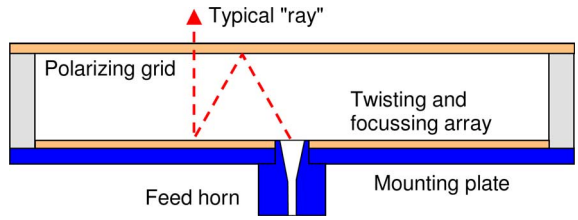

Fig. 1. Principle cross section and typical ray of a folded reflectarray antenna.

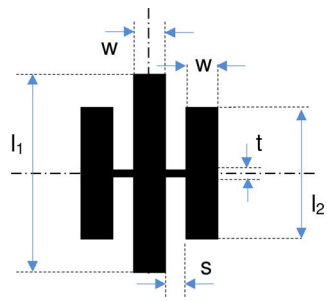

Fig. 2. Reflector element for the dual frequency reflectarray ($w = 0.5$ mm, $t = 0.3$ mm, $s = 0.3$ mm).

a 90° twisting of the polarization, so that the wave now can pass through the polarizing grid. For this, the elements of the reflectarray are oriented at 45° with respect to the polarization of the incident wave. Decomposing the electric field into two components parallel to the axes of the elements and adjusting a reflection phase difference of 180° between the two polarizations results in the required polarization twisting [10].

For a dual-frequency antenna, this principle has to be extended such that both the required reflection phase angles as well as the 180° phase angle difference are adjusted *independently* for the two frequencies. A further side condition for a simple and cost-effective configuration is the selection of a single-layer reflectarray substrate.

III. Dual-Frequency Reflector Elements

To fulfill the requirements as given above, elements are needed to resonate at two different independently adjustably frequencies. This principle is the basis of [8] and [9], and a number of alternative elements for single polarization have already been described in [11]. In that work, the double-frequency resonance (with both frequencies close together) has been used to provide a more wideband and flatter response for a single frequency band, but equally, the two resonances may be selected farther away from each other. For the antenna reported here, an element from [11] was selected (Fig. 2), printed on an RT Duroid 5880 substrate ($\varepsilon_r = 2.22$, substrate thickness 0.5 mm) with backside metallization.

With the typical approach, the behavior of the reflectarray elements is investigated using a periodic array of elements and a

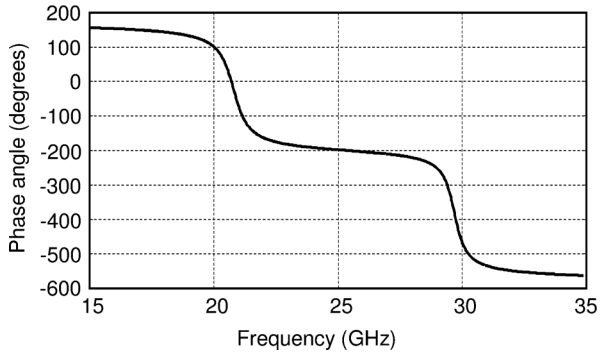

Fig. 3. Phase angle curve of the element in Fig. 2 for $l_1 = 5$ mm and $l_2 = 3.5$ mm.

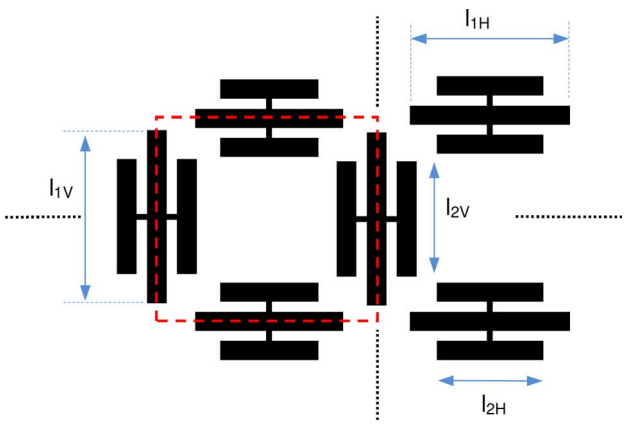

Fig. 4. Principle element structure and unit cell for the dual-frequency reflectarray. The planar structure is extended periodically into both directions.

normal incidence of a wave. Simulation is done with the CST Microwave Studio [12] (using the frequency-domain solver). Polarization is parallel to the vertical strips. The lengths l_1 and l_2 (see Fig. 2) are adjusted for the reflection phase angle of the lower and upper frequency band, respectively. Some interdependence of the angles is due to coupling of the strips. A typical reflection phase angle curve is plotted in Fig. 3. With a single-layer structure of the given thickness, about 330° of phase angle range can be covered at each frequency. A thinner substrate provides a wider range, but at the expense of very steep curves. Modifying lengths l_1 and l_2, the respective parts of the curve shift left or right.

For a first test, a reflectarray similar to that in [8], but for single polarization, was designed and tested, giving promising results (not reported here). Next, similar to [13], a combination of these elements in different directions has been investigated (Fig. 4). A quadratic unit cell is indicated by the dashed line in Fig. 4; the size of this cell has been selected to 7 mm. As mentioned for the structure shown in Fig. 2, the principle behavior of a periodic arrangement of such cells is simulated for an incident plane wave from broadside independently for both polarizations. Due to a double symmetry, only one quarter of the cell has to be computed.

Now, the four different strip lengths—horizontal and vertical orientation of the elements for horizontal and vertical polarization—have to be adjusted to provide a given reflection phase angle independently for each frequency with the side condition

TABLE I
ELEMENT DIMENSIONS FOR THE DIFFERENT PHASE ANGLE COMBINATIONS $(l_{1H}, l_{1V}, l_{2H}, l_{2V})$; SEE FIG. 4

30 GHz	20 GHz →			
↓	0°	90°	180°	270°
0°	(5.25, 5.58, 3.44, 3.69)	(5.19, 5.3, 3.44, 3.7)	(4.3, 5.08, 3.51, 3.69)	(5.31, 4.73, 3.44, 3.69)
90°	(5.16, 5.61, 3.39, 3.47)	(4.53, 5.31, 3.43,3.48)	(5.54, 5.18, 3.37, 3.48)	(5.31, 4.96, 3.38, 3.49)
180°	(5.08, 4.3, 3.69, 3.51)	(4.73, 5.31, 3.69, 3.44)	(5.58, 5.25, 3.69, 3.44)	(5.3, 5.19, 3.69, 3.44)
270°	(5.19, 5.54, 3.48, 3.37)	(4.96, 5.31, 3.49, 3.38)	(5.61, 5.16, 3.47, 3.39)	(5.31, 4.53, 3.48, 3.43)

that there is a 180° phase difference between horizontal and vertical polarization—once again separately at both frequencies. On the other hand, the unit cell should be reasonably small, so a coupling between all structures occurs that automatically is taken into account by the simulation of the periodic structure but, as a consequence, does not allow adjusting the four line lengths independently. For each polarization, phase curves very similar to those of Fig. 3 result, but changing, e.g., the lengths of the horizontal strips for horizontal polarization will also affect the phase curve of the vertical polarization.

To ease the array design, a Fresnel-type approach was selected with only four phase angle states, resulting in 16 different cell configurations. In a first step, all strip lengths were determined independently for the respective polarization, modifying only the particular line lengths and leaving the orthogonal line lengths at some more or less arbitrary value. This of course ignores that the phase behavior in the orthogonal polarization is modified to some extent as well. In a second step a manual optimization for all four line lengths follows correcting for the coupling and providing the four line lengths for the required phase angles at the two frequencies as well as the phase angle difference of 180°. The resulting dimensions are given in Table I.

IV. ARRAY DESIGN AND EXPERIMENTAL RESULTS

The diameter of the reflectarray was selected to 190 mm (180 mm covered effectively with reflection elements); the distance between reflectarray and polarizer is 60 mm resulting in a focal length of 120 mm. A circular feed horn of 12 mm aperture diameter (with a taper to K-band rectangular waveguide) is placed in the center of the reflectarray. The radiation diagrams of the horn were quite similar in both planes and provide an edge taper at the reflectarray of about 6 and 7 dB at 20 and 30 GHz, respectively (Fig. 5). Ray tracing was applied to determine the required phase angles at the two frequencies, and the element dimensions were selected (modulo 90°) from the precalculated data base (Table I). A section of the resulting layout is shown in Fig. 6, including the marker for the feed.

The polarizer is a simple printed grid (RT Duroid 5880, thickness 3.18 mm, line width 0.35 mm, center-to-center distance of lines 0.8 mm, metallization thickness 17 μm) and was taken from another antenna at 30 GHz, so it is perfect for the upper

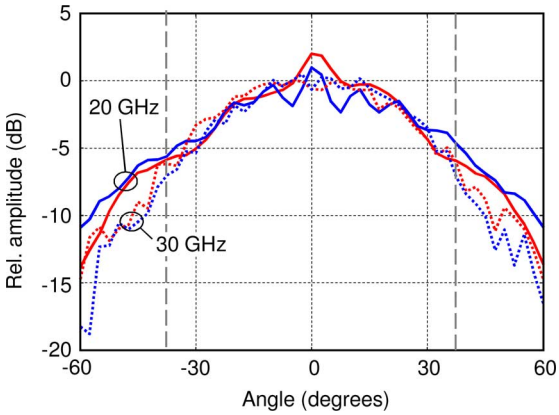

Fig. 5. Radiation diagrams of the feed horn (red: E-plane; blue: H-plane). Measurement was done with the horn mounted to the reflectarray plate (just removing the perspex ring and the polarization grid). Especially at 20 GHz, some interaction with the reflectarray occurs, and at 30 GHz, some noise can be seen. The dashed gray lines indicates the illumination edge of the antenna.

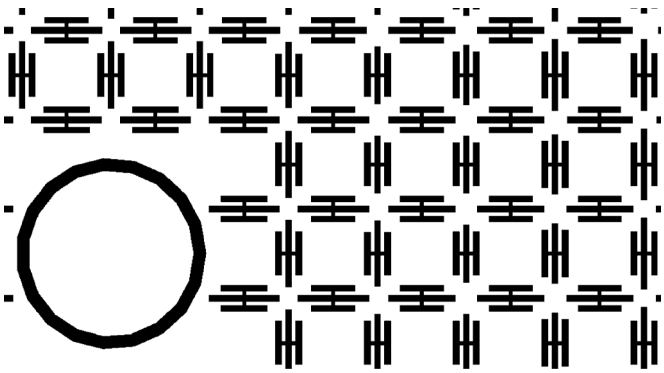

Fig. 6. Section of the reflectarray layout. The ring at the lower left is a marker for the feed position.

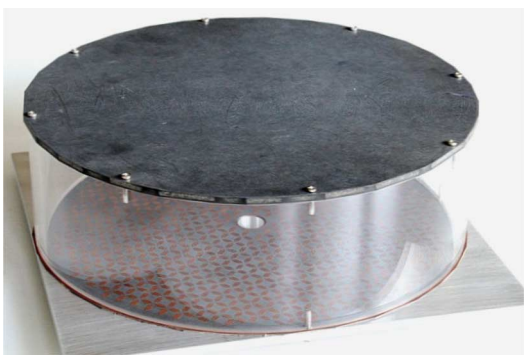

Fig. 7. Photograph of the realized antenna.

TABLE II
PERFORMANCE OF THE POLARIZING GRID (SIMULATED USING A MODE MATCHING APPROACH)

	20 GHz	30 GHz
Isolation (E-field parallel to grid)	25 dB	24 dB
Return loss (E-field normal to grid)	9.5 dB	38 dB
Insertion loss (E-field normal to grid)	0.52 dB	0 dB

frequency, but has some drawback at 20 GHz (see Table II). The grid is held by a perspex ring. A photograph of the antenna is shown in Fig. 7.

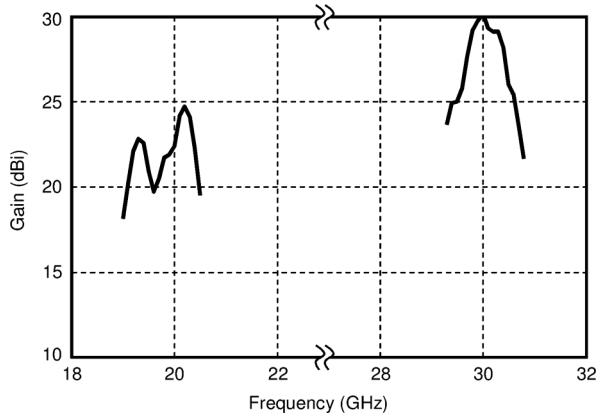

Fig. 8. Measured gain values of the antenna.

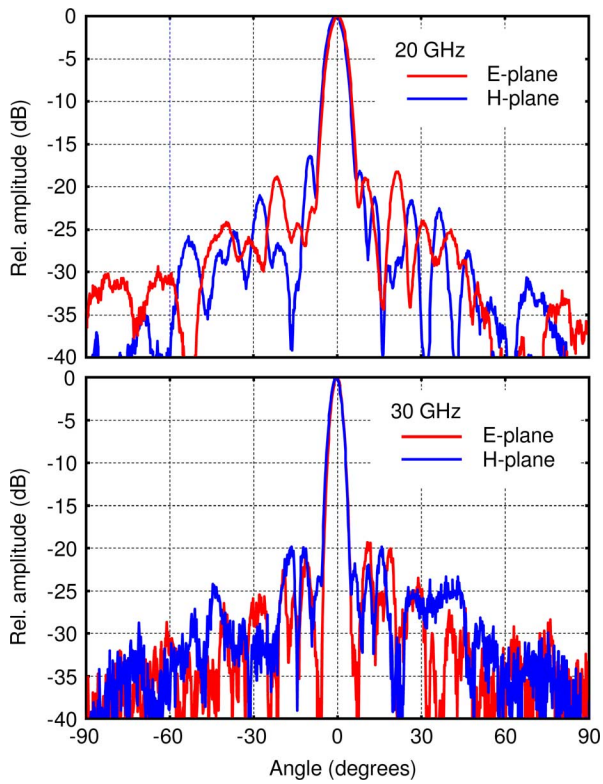

Fig. 9. E- and H-plane radiation diagrams at 20 and 30 GHz.

In a first test, the antenna was placed on the turntable in the anechoic chamber and adjusted for maximum amplitude (main beam), and the transmission between transmit antenna and the antenna under test was recorded as a function of frequency. These values then were compared to those of pyramidal horns at K- and Ka-band with approximately 20 dB of gain each. The respective results are plotted in Fig. 8. Maximum antenna gain is 25 and 30 dB at 20 and 30 GHz, respectively. The 3-dB bandwidth is in the range of 1 GHz; around 20 GHz, there is some resonance due to unwanted reflections of the polarizer grid not working perfectly at this frequency (which also reduces gain by at least 0.5 dB and slightly increases sidelobe level).

In a next step, radiation diagrams were measured at different frequencies; E- and H-plane diagrams at 20 and 30 GHz are plotted in Fig. 9. Diagrams very similar to these are maintained

TABLE III
SUMMARY OF ANTENNA RESULTS ($\Delta\Theta_E$, $\Delta\Theta_H$: BEAMWIDTHS IN E- AND H-PLANE, SLL_E, SLL_H: MAX. SIDELOBE LEVEL IN E- AND H-PLANE, η: APERTURE EFFICIENCY ($\eta = G(\lambda^2)/(4\pi A) = G((\lambda)/(\pi d))^2$, $d = 180$ mm)

	$\Delta\Theta_E$	$\Delta\Theta_H$	G_{max}	η	SLL_E	SLL_H
20 GHz	6.2°	6.2°	25 dBi	22.3 %	18 dB	16.5 dB
30 GHz	3.7°	4°	30 dBi	31.3 %	20 dB	20 dB

within a 1-GHz bandwidth. A summary of antenna performance is given in Table III. Compared to single-frequency folded reflectarrays, gain and efficiency are lower. About 1 dB of loss in gain results from the Fresnel approach [14], some loss also results from the relatively large cell size necessary to implement two sets of orthogonal elements, and at least 0.5 dB at 20 GHz are due to the insertion loss of the grid at that frequency. A major drawback is the small bandwidth, apparently due to the large unit-cell size and the use of narrow lines in the reflector elements. In this respect, a dual-layer substrate with wide rectangular elements may give a substantial improvement and also may exhibit results closer to those of [3]. This measure, however, would be taken at the expense of a more complicated fabrication process and higher cost for the material. Also, a more sophisticated polarizer (e.g., dual layer as well) would improve the performance at 20 GHz.

REFERENCES

[1] M. R. Chaharmir, J. Shaker, and H. Legay, "Dual-band Ka/X reflectarray with broadband loop elements," *Microw., Antennas Propag.*, vol. 4, pp. 225–231, 2010.

[2] C. Han, C. Rodenbeck, J. Huang, and K. Chang, "A C/ka dual frequency dual Layer circularly polarized reflectarray antenna with microstrip ring elements," *IEEE Trans. Antennas Propag.*, vol. 52, no. 11, pp. 2871–2876, Nov. 2004.

[3] J. A. Encinar and M. Barba, "Design manufacture and test of Ka-band reflectarray antenna for transmitting and receiving in orthogonal polarization," in *Proc. 14th ANTEM-AMEREM*, 2010, pp. 1–4.

[4] J. A. Encinar, M. Arrebola, L. F. de la Fuente, and G. Toso, "A transmit-receive reflectarray antenna for direct broadcast satellite applications," *IEEE Trans. Antennas Propag.*, vol. 59, no. 9, pp. 3255–3264, Sep. 2011.

[5] M. R. Chaharmir, J. Shaker, N. Gagnon, and D. Lee, "Design of broadband, single layer dual-band large reflectarray using multi open loop elements," *IEEE Trans. Antennas Propag.*, vol. 58, no. 9, pp. 2875–2883, Sep. 2010.

[6] D. Pilz and W. Menzel, "Printed millimeter-wave reflectarrays (invited)," *Ann. Télécommun.*, vol. 56, no. 1–2, pp. 51–60, 2001.

[7] A. Kohmura, J. Lanteri, F. Ferrero, C. Migliaccio, P. Ratajczak, S. Futatsumori, and N. Yonemoto, "Ka-band dual frequency switchable reflectarray," in *Proc. 6th EuCAP*, 2012, pp. 3230–3233.

[8] P. Grüner and W. Menzel, "Single-layer dual-frequency reflectarray," in *Proc. iWAT*, Karlsruhe, Germany, Mar. 4–6, 2013, pp. 318–321.

[9] B. Oulèye, J. Lanteri, C. Migliaccio, and W. Menzel, "Dual-band Fresnel reflector for communication UAV—satellite," in *Proc. 18èmes Journées Nat. Microondes* (in French), Paris, France, May 15–17, 2013, pp. 1–4.

[10] W. Menzel, D. Pilz, and M. Al-Tikriti, "Millimeter-wave folded reflector antennas with high gain, low loss, and low profile," *IEEE Antennas Propag. Mag.*, vol. 44, no. 3, pp. 24–29, Jun. 2002.

[11] S. Dieter, C. Fischer, and W. Menzel, "Single-layer unit cells with optimized phase angle behavior," in *Proc. 3rd EuCAP*, Mar. 23–27, 2009, pp. 1149–1153.

[12] CST Microwave Studio. ver. 2011, Computer Simulation Technology AG, Darmstadt, Germany, 2011.

[13] W. Menzel, J. Li, and S. Dieter, "Folded reflectarray antenna based on a single layer reflector with increased phase angle range," in *Proc. 3rd EuCAP*, Mar. 23–27, 2009, pp. 2757–2760.

[14] R. J. Mailloux, *Phased Array Antenna Handbook*, 2nd ed. Boston, MA, USA: Artech House, 2005.